Model of heterogeneous microscale in SOFI for Monte Carlo simulations

Nathan L. Gibson

May 21, 2007

Abstract

We present a methodology for creating a simulated foam microstructure for use in forward simulations of wave equations to quantitatively analyze the expected scattering phenomenon primarily responsible for the attenuation of interrogating signals in Sprayed-On Foam Insulation (SOFI). Our approach builds off of the popular use of Voronoi Tessalations for crystal growth modeling by using the Laguerre variant (Apollonius Graph) applied to close-packed spheres. A *filled-in* random raindrop algorithm is used to generate the packing configuration. Lastly, variation of diameter mean values is used to model knitlines, i.e., the interfaces between sprayed-on layers.

1 Introduction

Cellular structures are common in many materials including foam, metals, ceramics, magnetic and ferroelectric materials, fluids and even biological tissue [MS07]. Methodologies for properly modeling the heterogeneous structure of these materials will aid in the understanding of their mechanical and dielectric properties. Specific examples include low-loss, high dielectric constant materials which have applications in the design of circuit components and quasi-optical elements [BBR+03], and low (nearly constant) dielectric constant materials with high loss at infra-red frequencies which can be used as dichroic filter to transmit THz radiation with small losses [ZMWP02].

Our efforts herein are toward sufficiently modeling the heterogeneous microstructure of foam, particularly Sprayed-On Foam Insulation (SOFI), with an algorithm which can be used as part of a Monte Carlo simulation of pulse propagation through trial topographies in order to understand the effect of the cellular structure on the frequency dependent attenuation due to scattering. In particular, our algorithm can be used to generate random media satisfying given statistical characteristics. For each description of material produced, an interrogating pulse may be propagated numerically with the usual Maxwell's equations, and the results, for instance either loss tangent or backscatter, may then be correlated by some characterization of the media (e.g., average cell size or coefficient of variation). This understanding, in turn, could lead to improved (e.g., more accurate and/or efficient) models of scattering effects which are important in such areas as damage detection of Space Shuttle foam using THz pulse interrogation[XXZM04], and imaging of foam or froth-like materials in industrial or security applications.

An exact formula for the evolution of individual grains (which produce the cellular structure) in higher than two dimensions has recently been proposed [MS07]. Their formulation involves integral geometry and geometric probability, and may eventually lead to a more accurate, though likely more expensive, algorithm for generating simulated microstructures. This breakthrough further indicates the potential for the type of modeling approach described herein for analyzing the dielectric properties of complex microstructures.

1.1 Scattering

The fundamental aspect of modeling THz wave propagation in SOFI is correctly accounting for the frequency dependent attenuation due to scattering in the time domain. Most of the literature on scattering methods is either for the case where the product of the wavenumber k and the characteristic length scale of the material (cell size) a is very large or very small (see, for example, [Ish78]). For the region in between, there has been much work done in the time-independent case [CT98]. For ka large, there exist formulas for effective scattering and absorption coefficients in the time dependent case, but they involve opaque spheres [Bre04], not general mixtures of materials. However, these results were compared successfully to Monte Carlo simulations from [CB04]. Results of experiments specifically for THz frequency wave propagation, in this case through a collection of Teflon spheres, were also compared with Monte Carlo simulations [PM01]. The main thrust of that effort was to extract the scattering mean free path $l_s(\omega)$ over a broad bandwidth. The authors also report observing scattering-induced dispersive effects.

Labratory experiments have been performed to measure the dielectric constant and loss tangent of materials at THz frequencies [BBR+03, Con04]. Specifically for foam, THz dielectric properties, including the

extinction coefficient, were experimentally measured in [ZMWP02]. However, there were no simulations or modeling in these reports.

Our eventual goal is to understand the frequency dependence of the attenuation due to scattering in foam-like materials. As the amount of scattering is highly dependent on the dimensionless parameter ka, this will lead to a density dependence as well. A relationship between scattering and density would be helpful in accurately modeling knitlines in SOFI, but also possibly in determining bulk density of a high-contrast material based on backscatter.

1.2 Preliminaries on Structure of Foam

We assume that the foam under investigation is a binary mixture, meaning some solid substance (e.g., polyurethane) surrounding some gaseous blowing agent in a cellular structure. A sample prototype for foam microstructure is given by Figure 1, which shows SOFI under 25X magnification. The region with significantly smaller sized cells is actually the top of one sprayed-on layer that was allowed to cure momentarily before another layer was added upon it. The visible lines in the resulting cross-sections of foam are called "knitlines".

Characteristics of the microstructure which must be accurately represented by a model for use in a wave scattering simulation include the hexagonal pattern of the cells, the ratio of average cell size to wall thickness, the distribution of various cell sizes, the presence (if any) of knitlines, and the elliptical effect resulting from rising gases after spraying.

We will further assume that the material is non-polar, or rather that the polarization effects are neglibile compared to the attenuation due to scattering from interfaces. Therefore, in representing the microstructure in a simulation, it is sufficient to determine the frequency dependent speed of propagation of light in the solid substance as well as the gaseous filler, and provide an indicator function such that given a location in space, the indicator function will determine whether the point is inside the solid or gaseous substance. For the purposes of a discretization of the domain, this indicator function could be a matrix of say ones or zeros on some grid. In the development below we will assume that our domain is uniform in the y direction and thus essentially two dimensional. The general ideas will hold for a full three dimensional treatment, however two dimensions are sufficient for treating common geometric complexities such as curves, corners, and non-normal angles of incidence. Additionally, we will be able to make a direct comparsion to our prototypical example from Figure 1. It was shown in [ORTG00] that a 2D tessellation has simliar statistical and topological properties as those of a 2D slice of a 3D tessellation, thus we expect our 2D model to qualitatively represent the prototypical example.

2 Algorithm Development

In this section we describe the main ideas that went into the eventual modeling algorithm. We begin with the manner in which the cells are formed from a given arrangement of spheres, and then explain the generation of that arrangement. Next, we describe how the topological representation of the cells can be translated into a useable form in a simulation code, namely an indicator matrix. Finally we mention the procedure for modeling foam with elliptical cells on a possibly rectangular domain.

2.1 Apollonius Graph

In order to accomplish an underlying regular hexagonal structure, one may apply a Voronoi tessellation to the centers of an arangement of close-packed disks of a fixed diameter. In Figure 2 the Voronoi tesselation of a regular packing of circles is given. The Voronoi tesselation approach is commonly used in micromechanical modeling (for example, see [SG97] and [HRA05]) when polydispersity is not important.

In general, however, foams are random polydisperse materials, i.e., they contain cells of various sizes and shapes [Kra03]. A generalization of the Voronoi tesselation is the Apollonius graph (also known as a radical tesselation). It incorporates the distance from the surface of an object rather than the center. Thus, the variety of sizes of packed spheres is inherited by the resulting cells. Figures 3 and 4 depict the Voronoi diagram and the Apollonius graph for a random packing of disks (the 2D Apollonius Graphs library from CGAL was used in the creation of these graphs [KY06]). In the Voronoi diagram the cell size is roughly uniform despite the variety of disk sizes. One of the first to suggest using an Apollonius graph to determine the local arrangement around a volume particle was [GF82]. The work of [ATG$^+$94] first applied this idea to binary assemblies of discs. Later, a subset of these authors studied the statistical properties of radical tessellations of binary mixtures of spheres [GORT02]. The work of [FWZL04] extended this approach to

random diameters (i.e., a distribution of spheres) producing what they called a RCP-LV diagram: "Voronoi diagram in the Laguerre geometry based on random closed packing of spheres." The authors note that the LV diagram preserves the distribution of sphere diameters so that the resulting cellular volume distribution may be made to be log-normal as seen in experimental surveys of real foam. This is opposed to the Poisson-Voronoi diagram (PV), in which volumes obey a gamma distribution. Further, the PV diagram results in an invariant constant of variation (CV) which is much lower than that which is physically observed for foam in nature.

2.2 Sequential Generation

The RCP-LV algorithm, however, relied on a rearrangement process for the generation of close-packed spheres, as opposed to sequential generation such as Random Sequential Adsorption (RSA) [Fed80]. In a rearrangement algorithm the structure of a regular packing (e.g., body centered cubic BCC, or face centered cubic FCC) is made random by perturbing the x, y and z coordinates of the centers of the spheres by a trial value which is distributed randomly, say with a standard deviation equal to a fixed scaling factor times the diameter of the sphere (i.e., a fixed coefficient of variation). Alternatively, RSA chooses x, y and z coordinates along with a radius r from some appropriate distribution and attempts to place the sphere in the domain. If there is any overlap with an existing sphere, the new sphere is discarded and another trial is attempted. The jamming limit is reached when no new spheres may be placed.

There is still some debate as to which approach one should use for generating a truly random close-packing of spheres, or even if the problem is well-defined [TTD00]. For our purposes, the method of "drop and roll," a sequential algorithm introduced by [VB72], is the only one with the (possibly) desired characteristic that all spheres are touching other spheres. Additionally, the resulting packing ratio of .6 (considerably higher than that achievable with RSA) is sufficient to accentuate the inheritance of polydispersity in the packed spheres to the tessellation [ATG$^+$94]. The sequential generation algorithms as a whole are prefered over randomly distorted regular packings (rearrangement) as the latter severely restricts the polydispersity [HRA05]. An example of the output of the "drop and roll" algorithm is shown in Figure 5 (the FORTRAN code MAP_POLY_DROPS [Car97] was used in generation of these plots). In two dimensions, the x coordinate is chosen from a uniform distribution, and the diameter of the disk is log-normally distributed. The disk is "dropped" from a height well above the other disks until it makes contact. The disk then "rolls" along the surface of the other disk until contact with a third disk is made. If it is determined that the disk may continue to roll, the process is repeated. Otherwise, movement terminates and the position is fixed.

We have additionally *filled-in* any remaining holes down to an minimum acceptable size. This procedure is made remarkably efficient by the double use of the Apollonius graph. The Apollonius graph can be used to construct an arrangement of circles such that the vertices of the graph are the centers of the circles, and the distances from these vertices to the three nearest disks (drops) form the radii of the circles. In essence, the Apollonius graph determines the "kissing circles" of any three neighboring disks. If the diameter of this kissing circle is sufficiently large, it may be added to the original arrangement of disks. It will be guaranteed to be touching other disks but not overlapping. Thus, given the Apollonius graph, we construct the descriptions of these kissing circles and sort them in order of increasing radius. Sequentially, the circles with radii sufficiently large (e.g., within one or two standard deviations of the mean) are added to the packing. Each circle must only be determined to not overlap with a previously added kissing circle. After all circles have been added, the Apollonius graph is reconstructed. There are incremental algorithms that would further exploit this approach by simply modifying the original graph. However, we have not implemented this here. Figure 6 shows the filled-in version of the Apollonius graph from Figure 5. Disks numbered 55 through 62 have been added to fill gaps, including number 57, which extends beyond the boundary of the bin. The choice whether or not to allow these extensions is arbitrary as usually the cells near the boundary are truncated anyway.

Of all of the possible combinations of the several tessellation algorithms and the many more circle/sphere packing algorithms, it seems that this particular combination of the Apollonius Graph applied to a "drop and roll" sequential generation algorithm has not yet been studied. And yet, for the reasons described above, it is the single combination that seems to have the desired properties for efficiently and effectively representing the characteristics that are important to analyzing electromagnetic scattering in the microstructure. It should be pointed out that none of the above references were concerned with scattering effects. Instead, they focused on either topological properties of packings or microstructure, or else mechanical properties of foam via simulations (in addition, see [RG01]). This is a significant difference in that, for example, the Voronoi tessellation gives the usual 120° at edge intersections which is crucial to the mechanical structure

of the foam. The Apollonius graph does not guarantee this property. However, it is arguably less important to wave scattering.

Figure 7 shows the final result of applying the Apollonius graph to the filled-in "drop and roll" disks. In order to neglect boundary effects, the graph is truncated a distance of two mean diameters from the boundary of the bin. For some applications it may be desirable to retain at least one boundary (for example foam affixed to an aluminum backing in the Space Shuttle problem), therefore the x-axis has not been removed in this example.

2.3 Indicator matrix

In order to use the microstructure developed by the algorithm inside a code for wave propagation, we must be able to convert the collection of lines from the Apollonius graph into a matrix of zeros and ones which indicate whether there is a cell wall inside the corresponding element of the discretized mesh (e.g., finite element). This conversion must take into account the desired thickness of the cell walls (relative to the unit reference area). An example is given in Figure 8, where the thickness is given as .02. For each variation of the Voronoi tessellation, one must compute the corresponding indicator matrix which represents how the material would be represented in an actual simulation. Thus the Apollonius graph should be considered to be plotting the centerline of the cell walls.

Note that the thickness of the cell wall can easily be changed in the algorithm. One can also increase the refinement of the underlying grid. These parameters, along with the mean diameters of the disks (and therefore roughly the distribution of the diameters of the cells), must all be determined with respect to the unit reference area for the given application.

2.4 Rectangular domains and elliptical cells

In order to have any arbitrary sized rectangular domain, rather than a unit reference square, we must be able to scale differently the number of cells in the x direction from the z direction. This is done by changing the dimensions of the boundary bin in the "drop and roll" algorithm.

However, the problem of having elliptical cells is different. This requires a scaling after the tessellation on circular disks has been computed. Figure 9 gives an example of a material which has twice as many cells in the x direction as in the z direction. However, the diameter in the z direction is three times as large.

3 Foam and SOFI with Knitlines

Nearly all of the characteristics of the microstructure which must be accurately represented by a model for use in a wave scattering simulation which were mentioned above, are accounted for in the procedure we have described. In order to generate a model of the prototypical example from Figure 1 we must account for the stretching of cells in the z direction due to the rising of gases after spraying. We assume that the diameters are log-normally distributed with a mean diameter of around .02 with respect to a unit square domain, and that the z-axis is truncated to allow one third the number of disks vertically as horizontally. We compute the corresponding Apollonius graph of the resulting close packing of disks, and stretch this graph by a factor of 3 vertically to allow for the rising of gases. Finally we convert the graph to a 550×700 indicator matrix which is depicted in Figure 10.

The last of the characteristics desirable to represent is the presence of knitlines in the SOFI. We may model this by using a periodic, i.e., alternating, mean value for the diameter of the disks. For the region of large cells, a large value for the mean is used, and inside the region of the knit lines, a significantly smaller value is used. The coefficient of variation is constant throughout. The relative widths of each layer are determined by the periodicity, for example, 1000 large disks followed by 500 smaller disks, or possibly 10 rows of large disks followed by 4 rows of smaller ones, where the number of disks per row is determined by the size of the boundary bin and the mean value of the diameters. This latter choice of parameters was used to generate the indicator matrix depicted in Figure 11. The bottom half of the figure is identical to that of Figure 10, but the presence of the knitline is clearly visible in the middle of the domain. Each of these two plots took less than one minute to produce on a 3 GHz desktop computer.

There are many modifications that could be done to make the model presented here even more representative of a particular structure. For instance, in [VB72] a modification to the "drop and roll" algorithm is described which simulates shaking. This would have the effect of flattening a region of disks. This would be useful, for instance, on the top few rows of the larger disks before the smaller ones are dropped so that

the resulting knitline has less roughness. Other improvements include some continuous representation of the diameter mean values, rather than piece-wise constant.

4 Conclusions

Applying the algorithm for computing the Apollonius graph of circles resulting from the filled-in "drop and roll" sequential generation of disks, which have diameters log-normally distributed, gives an efficient model of the microstructure of foam. Additionally, using a variable mean value for the diameters of the disks provides a mechanism for introducing knitlines which occur at the top of each layer of sprayed-on foam. The resulting graph is converted into an indicator matrix which can be used inside a forward simulation of wave propagation through the cellular material to analyze the effect on scattering due to topological characteristics of the microstructure. Monte Carlo simulations may be used to understand the bulk scattering effects, give insight into a suitable homogenization formula, or to validate a proposed formula.

References

[ATG+94] C. Annic, JP Troadec, A. Gervois, J. Lemaître, M. Ammi, and L. Oger. Experimental study of radical tesselations of assemblies of discs with size distribution. *J. Phys. I France*, 4:115–125, 1994.

[BBR+03] P.H. Bolivar, M. Brucherseifer, J.G. Rivas, R. Gonzalo, I. Ederra, A.L. Reynolds, M. Holker, and P. de Maagt. Measurement of the Dielectric Constant and Loss Tangent of High Dielectric-Constant Materials at Terahertz Frequencies. *IEEE TRANSACTIONS ON MICROWAVE THEORY AND TECHNIQUES*, 51(4), 2003.

[Bre04] Q. Brewster. Volume scattering of radiation in packed beds of large, opaque spheres. *Journal of heat transfer*, 126(6):1048–1050, 2004.

[Car97] S. Cardie. Map_poly_drops. In Materials Algorithms Project, editor, *Materials Algorithms Project Program Library*. 1997.

[CB04] R. Coquard and D. Baillis. Radiative characteristics of opaque spherical particles beds: a new method of prediction. *Journal of Thermophysics and Heat Transfer*, 18(2):178–186, 2004.

[Con04] G.E. Conklin. Measurement of the Dielectric Constant and Loss Tangent of Isotropic Films at Millimeter Wavelengths. *Review of Scientific Instruments*, 36(9):1347–1349, 2004.

[CT98] P. Chiappetta and B. Torresani. Some approximate methods for computing electromagnetic fields scattered by complex objects. *Measurement Science and Technology*, 9(2):171–82, 1998.

[Fed80] J. Feder. Random sequential adsorption. *J. Theor. Biol*, 87(87):237, 1980.

[FWZL04] Z. Fan, Y. Wu, X. Zhao, and Y. Lu. Simulation of polycrystalline structure with Voronoi diagram in Laguerre geometry based on random closed packing of spheres. *Computational Materials Science*, 29(3):301–308, 2004.

[GF82] B.J. Gellatly and J.L. Finney. Characterisation of models of multicomponent amorphous metals: the radical alternative to the Voronoi polyhedron. *J. Non-Cryst. Solids*, 50(3):313–329, 1982.

[GORT02] A. Gervois, L. Oger, P. Richard, and J.P. Troadec. Voronoi and Radical Tessellations of Packings of Spheres. *Proceedings of the International Conference on Computational Science-Part III*, pages 95–104, 2002.

[HRA05] S. Hallström and S. Ribeiro-Ayeh. *Sandwich Structures 7: Advancing with Sandwich Structures and Materials*, chapter Stochastic finite element models of foam materials, pages 935–943. Springer, 2005.

[Ish78] A. Ishimaru. *Wave propagation and scattering in random media*. Academic Press New York, 1978.

[Kra03] A.M. Kraynik. Foam Structure: From Soap Froth to Solid Foams. *MRS Bulletin(USA)*, 28(4):275–278, 2003.

[KY06] M. Karavelas and M. Yvinec. 2d apollonius graphs (delaunay graphs of disks). In CGAL Editorial Board, editor, *CGAL-3.2 User and Reference Manual*. 2006.

[MS07] R. MacPherson and D. Srolovitz. The von neumann relation generalized to coarsening of three-dimensional microstructures. *Nature*, 446, 2007.

[ORTG00] L. Oger, P. Richard, J.P. Troadec, and A. Gervois. Comparison of two representations of a random cut of identical sphere packing. *The European Physical Journal B-Condensed Matter*, 14(3):403–406, 2000.

[PM01] J. Pearce and D.M. Mittleman. Propagation of single-cycle terahertz pulses in random media. *Opt. Lett*, 26:2002–2004, 2001.

[RG01] A.P. Roberts and E.J. Garboczi. Elastic moduli of model random three-dimensional closed-cell cellular solids. *Acta Materialia(USA)*, 49(2):189–197, 2001.

[SG97] M.J. Silva and L.J. Gibson. The effects of non-periodic microstructure and defects on the compressive strength of two-dimensional cellular solids. *International Journal of Mechanical Sciences*, 39(5):549–563, 1997.

[TTD00] S. Torquato, T.M. Truskett, and P.G. Debenedetti. Is Random Close Packing of Spheres Well Defined? *Physical Review Letters*, 84(10):2064–2067, 2000.

[VB72] W.M. Visscher and M. Bolsterli. Random packing of equal and unequal spheres in two and three dimensions. *Nature*, 239(5374):504–507, 1972.

[XXZM04] J. Xu, S.W. Xie, X.C. Zhang, and E. Madiras. T-rays identify defects in insulating materials. *Conference on Lasers and Electro-Optics (CLEO)*, 1:2, 2004.

[ZMWP02] G. Zhao, M. Mors, T. Wenckebach, and P.C.M. Planken. Terahertz dielectric properties of polystyrene foam. *Journal of the Optical Society of America B*, 19(6):1476–1479, 2002.

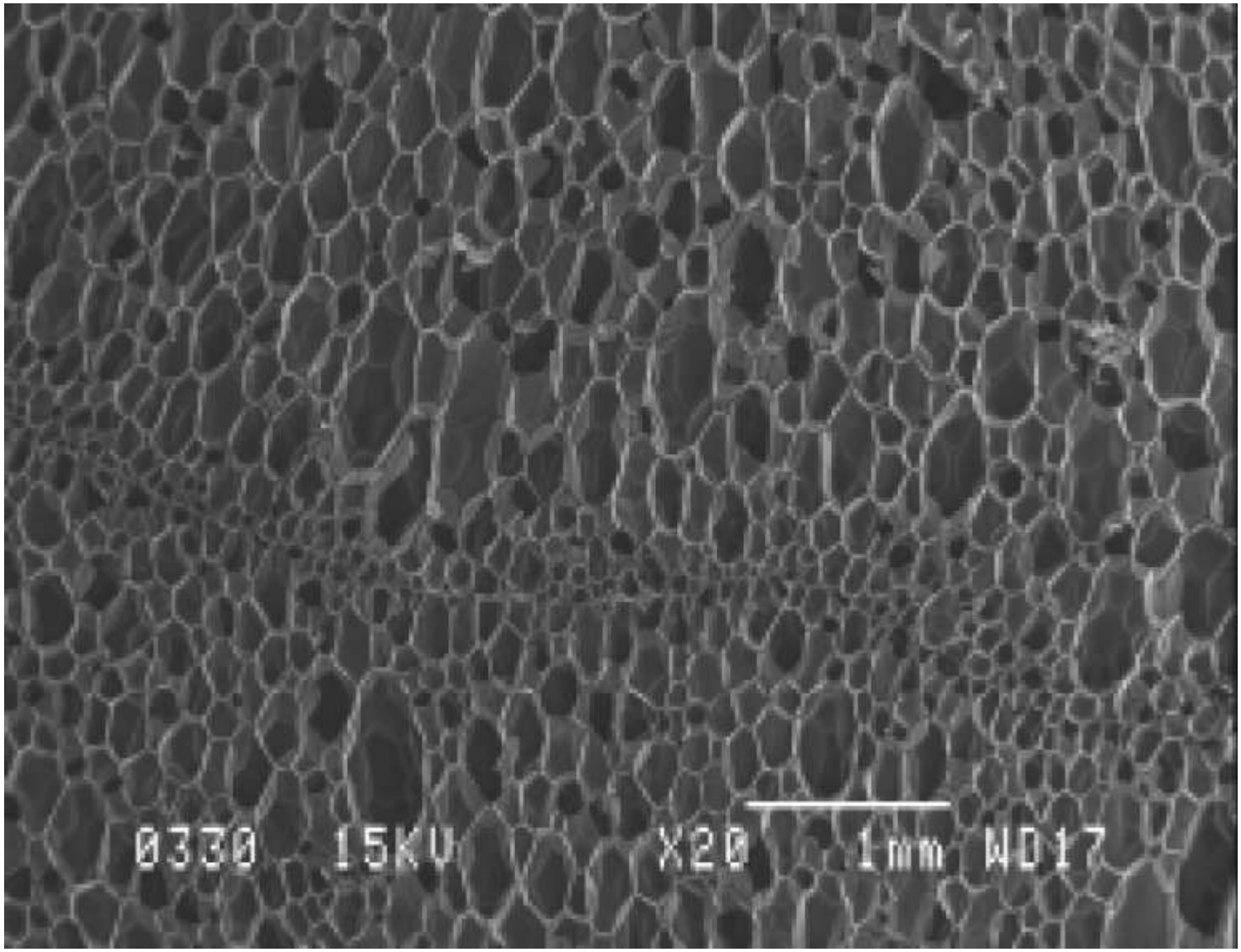

Figure 1: SOFI under 20X magnification

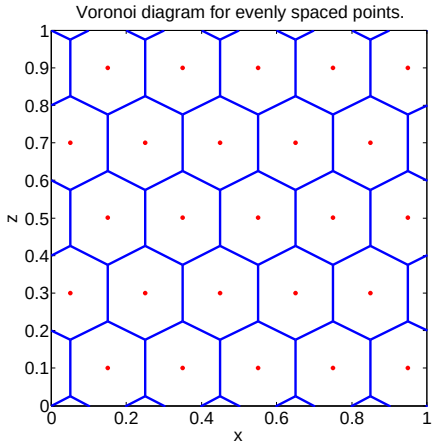

Figure 2: Voronoi tessellation of evenly spaced points.

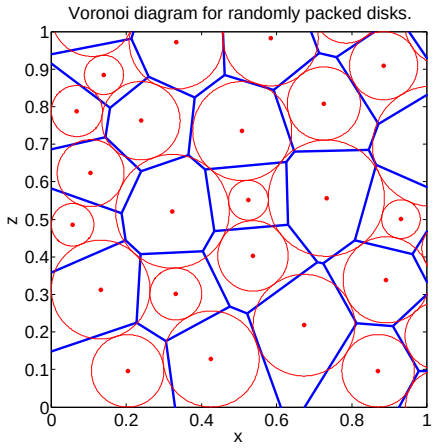

Figure 3: Voronoi tessellation of (the centers of) randomly packed disks.

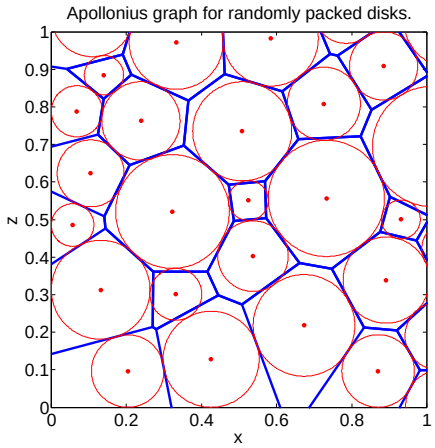

Figure 4: Apollonius graph of randomly packed disks.

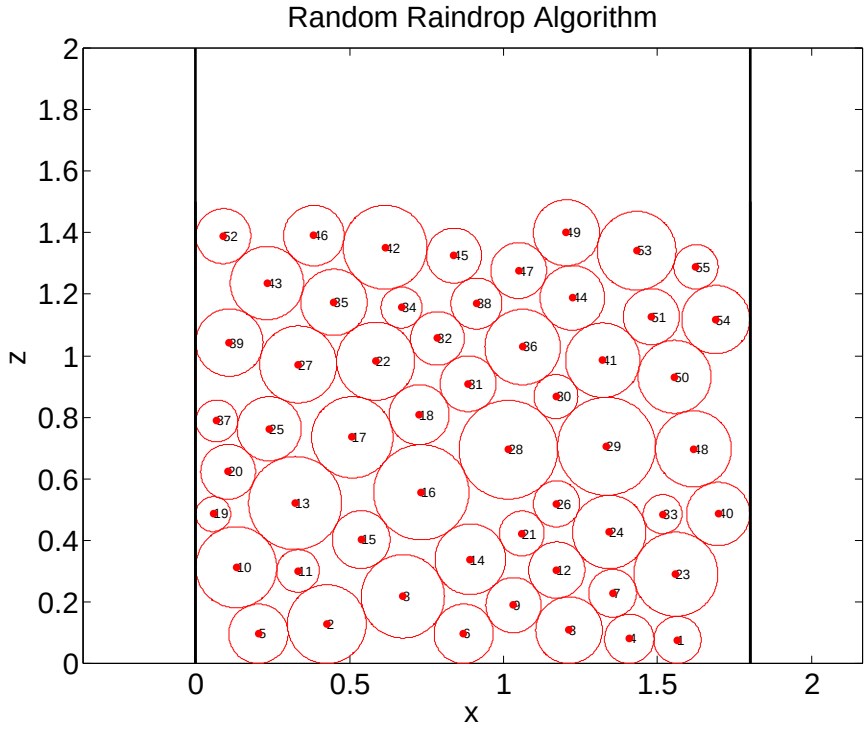

Figure 5: An example of the random raindrop or "drop and roll" algorithm for generating randomly close packed disks.

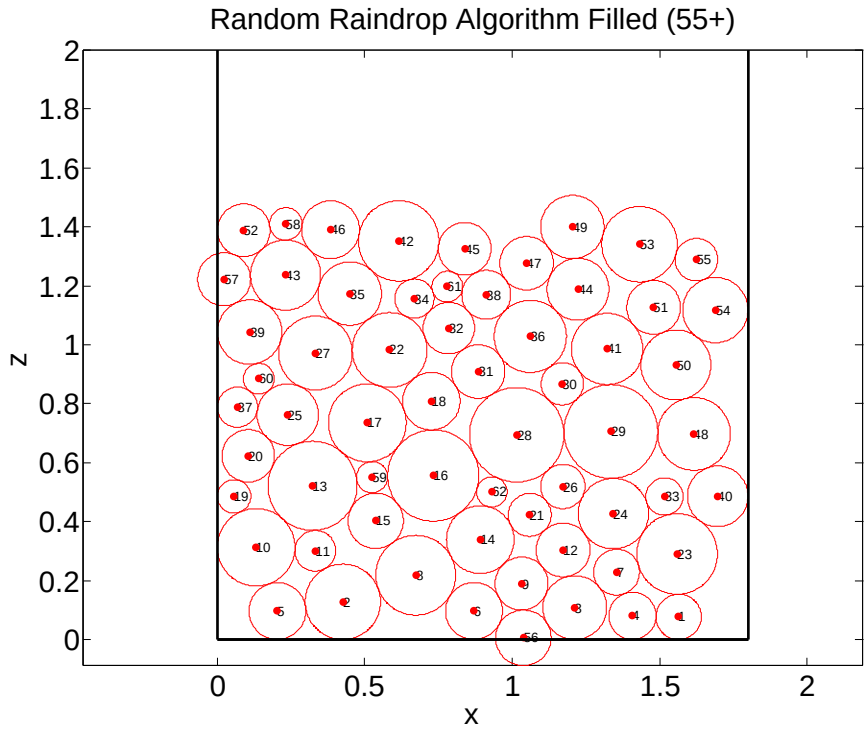

Figure 6: The "drop and roll" algorithm filled-in with disks of diameter at least the mean value minus two standard deviations (disks labeled 55 through 62 in decreasing order of size).

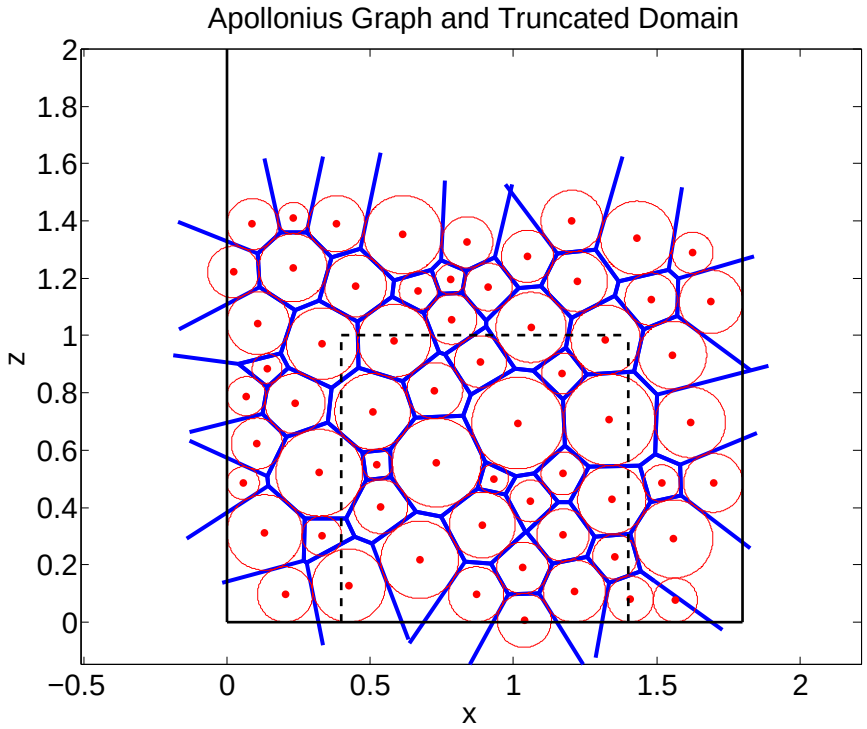

Figure 7: Apollonius graph on randomly close packed disks with a truncated domain indicated.

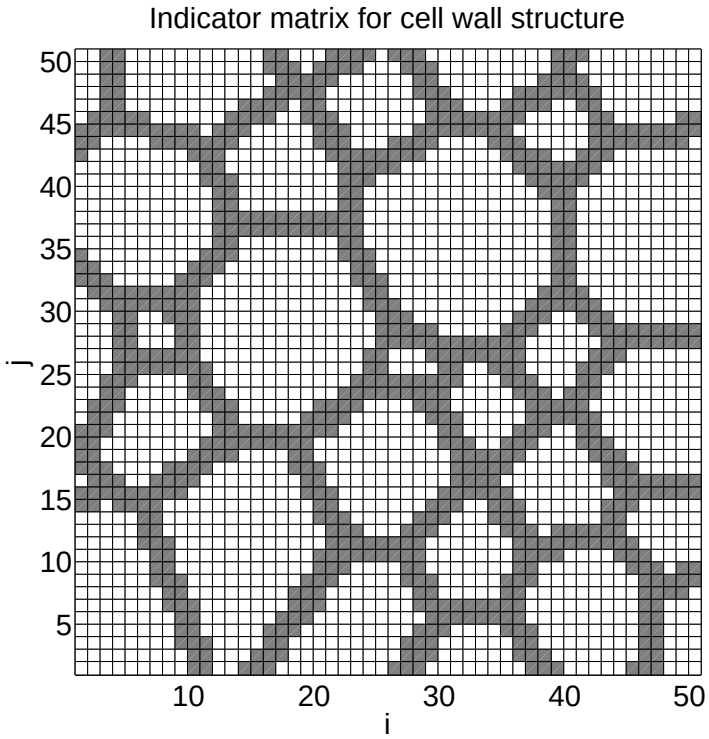

Figure 8: Indicator matrix for cell wall with thickness $2h$ where h is the meshsize.

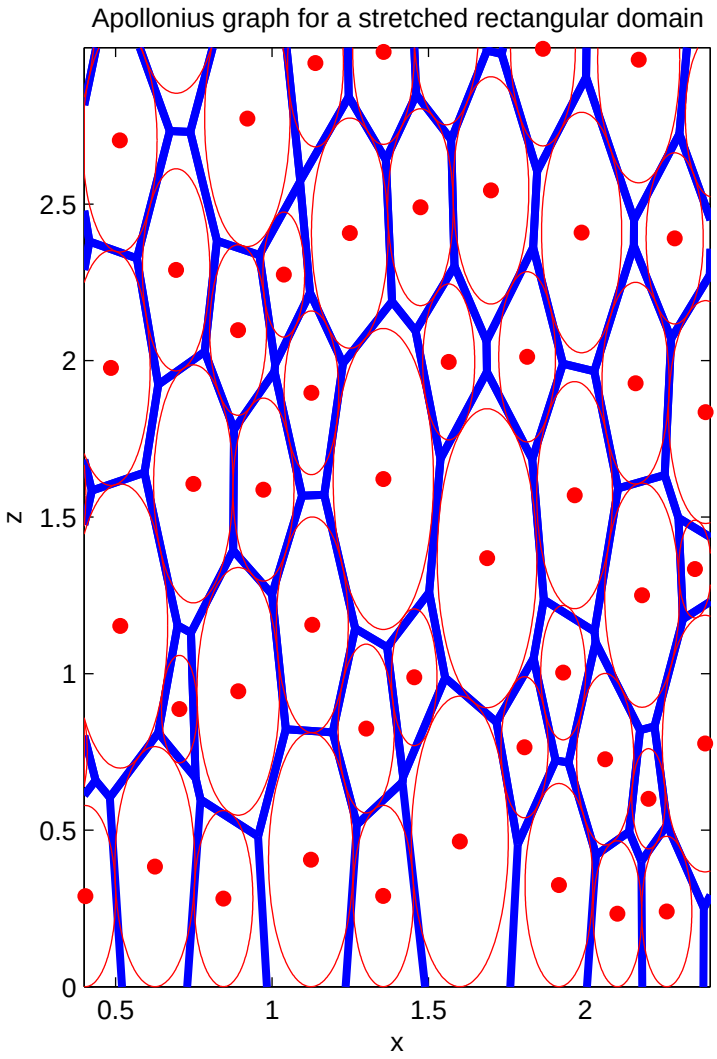

Figure 9: Apollonius graph for randomly packed elliptical cells on a rectangular domain.

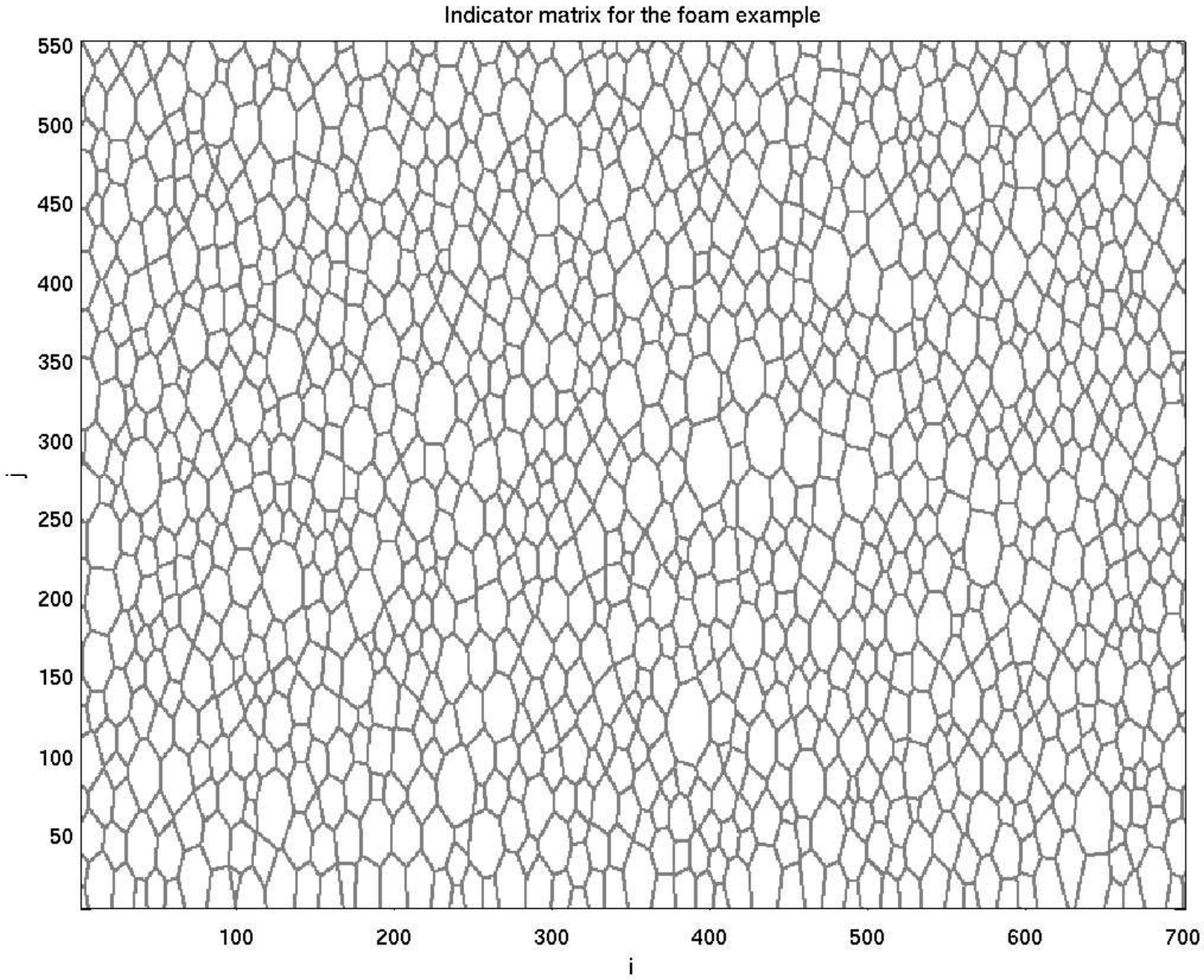

Figure 10: Indicator matrix for model of foam microstructure.

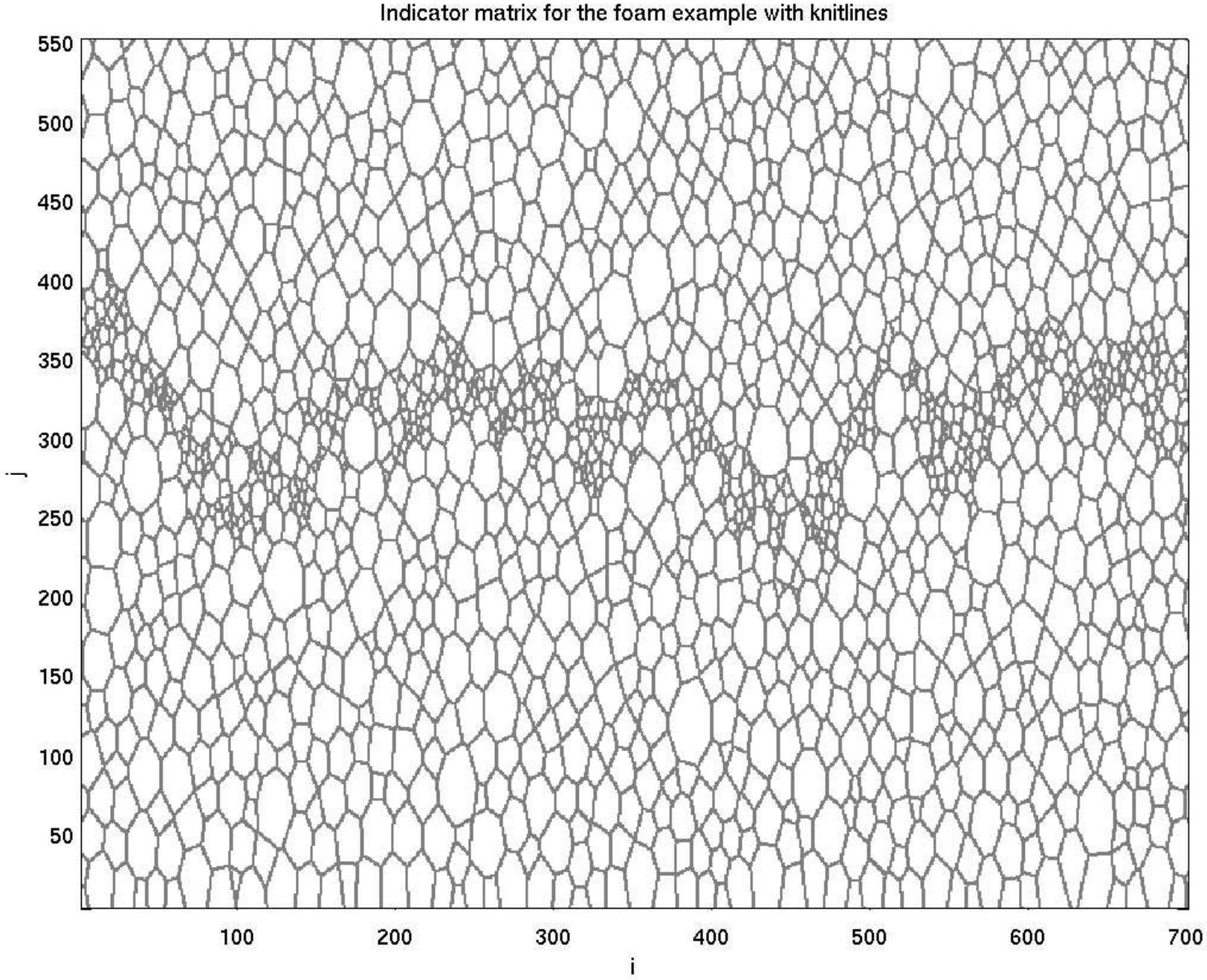

Figure 11: Indicator matrix for model of foam microstructure with knitlines.